Pitfalls in Using Pallor of the Eye to Detect Anaemia with Digital Cameras

Thomas A. Wemyss
Department of Medical Physics and Biomedical Engineering, University College London,
London, United Kingdom
rmaptaw@ucl.ac.uk

Ranjan Rajendram
Institute of Ophthalmology, University College London,
London, United Kingdom
ranjan.rajendram@ucl.ac.uk

Terence S. Leung
Department of Medical Physics and Biomedical Engineering, University College London,
London, United Kingdom
t.leung@ucl.ac.uk

***Abstract*— Anaemia - a reduced concentration of functional haemoglobin in the blood - affects around 20% of the global population. As a result, there is focus on developing non-invasive methods to screen for anaemia. A promising group of techniques uses smartphone imaging of external tissues. Because haemoglobin preferentially reflects red light, by measuring the colour ('redness') of blood vessels (or tissues as a whole), it is suggested that blood haemoglobin may be estimated. However, a potential issue is that 'redness' might depend not just on the severity of anaemia, but also upon the 'physiological structure' – i.e. the vessel density, vessel depth, and vessel diameter. We performed Monte-Carlo tissue optics simulations to investigate the potential impact of these structural factors on measurement of colour in the scleral conjunctiva. We found that within reasonable ranges of physiological structure, it is possible to get similar redness between severely anaemic (2.35 g/dL) and non-anaemic (15 g/dL) blood haemoglobin concentrations. This suggests that simple measurement of the redness of external tissues may not be suitable for detecting anaemia.**

***Clinical Relevance*— Pallor of external tissue is commonly used as a hallmark of anaemia. These results suggest that pallor may arise not only from anaemia, but also from variation in the physiological structure of the eye.**

I. Introduction

Anaemia affects more than 2 billion people and is characterised by a low concentration of functional haemoglobin within the blood [1]. Access to care remains a major challenge in the eradication of anaemia, and improved diagnostics could help address this problem [2].

Pallor – a characteristic paleness of external tissues – is a clinical sign of anaemia [3]. When screening for anaemia, the palm, conjunctiva of the lower eyelid, and nailbed are commonly examined – although a meta-analysis suggested that this tool is not as clinically sensitive as a blood test [4]. Particularly for mild anaemia, using pallor to judge anaemia can be challenging. Sensitivity and specificity of using pallor to detect mild anaemia have been reported below 75% [5], which is unlikely to be clinically useful as a singular tool for diagnosis [6]. When detecting severe anaemia, judgement of pallor is more likely to be accurate [7], but overall performance and inter-observer variability remain issues [8]. Using an objective measuring tool to measure colour to quantify pallor might improve this situation.

Smartphone colorimetry has become an emerging technique for non-invasively screening for anaemia, by predicting blood haemoglobin concentration using the colour of external tissues. This can be carried out on the nailbed [9] or on other areas with limited pigmentation, such as the sclera, with generally mixed performance [10], [11], [12]. Most techniques have three main steps: they firstly adjust for varying ambient lighting, after which they select pixels of interest, and finally they extract a 'redness measure' from which haemoglobin can be predicted.

Many of these smartphone colorimetry techniques involve measuring the colour of the vasculature on the eyelid, or the anterior segment of the eye. For example, [13] showed good performance screening for anaemia by identifying vessels in images of the sclera and extracting 'redness metrics' such as erythema index (a log of the ratio of red to green in the image). Other techniques implicitly extracted the pixels containing vessels – for example, by selecting the reddest pixels on the sclera [11].

The general principle underlying this colorimetry is that when the concentration of a protein containing a chromophore (such as haemoglobin in anaemia) or a pigment (such as bilirubin in jaundice) is altered, the attenuation coefficient μ of the blood or tissues changes. If the illumination and material thickness remain the unchanged, then any change in the output spectral power distribution can be attributed to this altered attenuation coefficient. This allows working backwards to estimate the underlying concentration of the pigment. In anaemia, the pigment of interest is haemoglobin itself, which has a characteristic high reflectance in the red wavelengths of light.

In physiological materials, the attenuation coefficient μ is the result of two separate processes within the material, absorption (represented by absorption coefficient μ_A) and scattering of photons (represented by the scattering coefficient, μ_S). In the simplest case of a pigment which is uniformly distributed throughout a medium, the attenuation coefficient μ_A can be expressed in terms of the molar concentration of the pigment c, and an intrinsic property of the pigment called the molar extinction coefficient ε:

$$\mu_A = \ln(10)\varepsilon c \quad (1)$$

The absorption coefficient μ_A represents a scale factor influencing the probability of a photon being transmitted, P(T), after a path length L as per Eq. (2):

$$P(T) = \exp(-\mu_A L) \quad (2)$$

Path length variation, for example due to changes in vessel diameter, as well as variations in μ_A and μ_S due to other chromophores, will therefore influence the observed colour. This means that the measured colour may not depend primarily on the concentration of haemoglobin, but also on the vessel diameter and tissue composition.

II. Factors Affecting Redness of Ocular Vessels

As shown in Fig. 1, redness of the sclera can vary even within the same participant. The aim of this work is to investigate the relative effects of haemoglobin concentration, vessel diameter, and other relevant physiological factors on the redness of the sclera, using a Monte-Carlo-based scleral colour model.

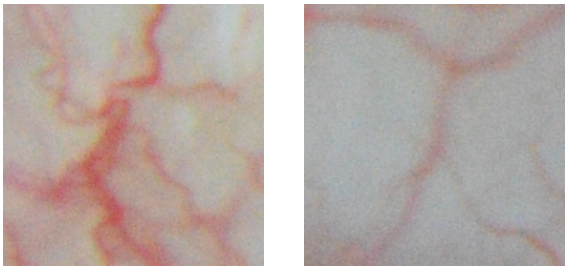

(A) (B)

Figure 1. Two images of the same sclera of one participant. (A) appears redder than (B) from increased vessel density and more superficial vessels.

A. *Vessel diameter*

Within each eye, there are a wide range of vessel diameters – likely from around 10µm [14] up to at least 250 µm. In previous research, assumptions have typically been made that vessel diameter, averaged over the entire sclera, would be comparable between participants, except in cases where there were specific, obvious confounding factors such as conjunctivitis [11]. However, there is a substantial body of evidence to suggest that capillary diameter in external tissues can vary with hypertension – for example, during pregnancy [15]. The pressure within the capillary might also vary with temperature [16], which might lead to a resultant change in the capillary diameter due to the force on the vessel wall.

Since Equation 2 establishes that light transmission depends on both μ_A (which depends on concentration of haemoglobin) and L, an objective of this research is to measure the relative magnitude of colour change from variations in μ_A and L, to determine whether changes in vessel diameter might be confused with changes in haemoglobin concentration.

Vessel diameter may be especially important because it does not only affect path length L, but there are also additional small-scale fluid-dynamic effects affecting μ_A. In whole blood, absorption of haemoglobin may not behave as in a homogeneous solution due to the pigment packaging effect [17]. The pigment packaging effect arises because haemoglobin in blood is packaged in high concentrations within red blood cells and is at virtually nil concentration within the plasma. This pigment packaging means that the overall absorption of the blood is slightly reduced – although this effect has only a small magnitude. Furthermore, the local concentration of haemoglobin may be reduced in small vessels compared to the circulatory system as a whole, due to the Fåhræus effect [18], [19]. The Fåhræus effect describes reductions in the local concentration of haemoglobin in narrow vessels due to the formation of a red blood cell-free boundary layer around the edges of the vessel, which makes up a significant proportion of the cross-section of some vessels in the microvasculature

B. *Vessel density*

Vessel density is a commonly used metric which quantifies the proportion of a volume which is occupied by blood vessels [20]. In the case of the sclera, we might consider a simplified version of vessel density, defined as the proportion of the area of the sclera which is covered with visible blood vessels. This would depend upon both the number of vessels, and the diameter of vessels. A greater vessel density might lead to a greater average redness of the sclera, even if blood haemoglobin remains the same.

C. *The sclera as an absorbing and scattering medium*

The sclera consists of intertwined collagen fibrils, each of which has a diameter of between 25 and 230nm [21]. These fibrils both scatter and absorb light. This means that the depth of blood vessels within the sclera will affect the spectral power distribution of the light returned from them. The episclera (the outer layer of the sclera) is particularly vascular, which means many vessels are superficial, but vessels may also lie within the deeper scleral stroma [22], [23].

It is also possible to observe brown pigmentation on the sclera, particularly with age, darker skin, or sun exposure [24]. It's likely that this pigmentation is primarily due to melanin, although it may also be due to scleral thinning or other physiological factors [25]. Melanin molecules reflect more light at longer wavelengths (within the visible wavelength range), meaning they preferentially reflect red light. Therefore, this pigmentation might affect the redness of the sclera.

III. Methods

This study was approved by the Local Ethics Committee for the UCL Department of Medical Physics and Biomedical Engineering (23447/002). Simulations were performed using Monte Carlo eXtreme [26], [27], [28]. Data analysis was performed in MATLAB R2024a.

A. *Simulation procedure*

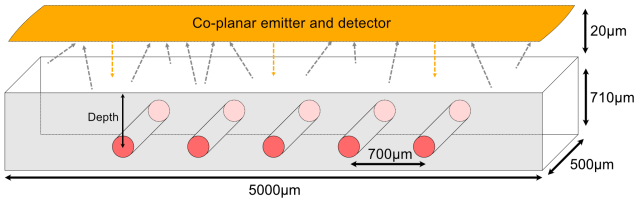

Figure 2. Geometry of Monte-Carlo simulation. Orange arrows represent example photon paths from the emitter. Grey arrows represent examples of returning photon paths, after scattering within the medium. The sclera/scattering medium is represented as a grey/white cuboid. Blood vessels are shown as red tubes. The depth parameter for each blood vessel (as well as the radius of the blood vessel) was configurable.

Simulation geometry is presented in Fig. 2. The sclera was simulated as a 710µm thick plane within a finite volume 5,000µm wide, 500µm tall and 750µm deep. Voxel size was set to 10µm. The phantom was illuminated at the normal to the surface by a pencil light source with the spectral power distribution of the CIE D65 illuminant. A circular photon detector with radius 50 µm was placed 20 µm above the planar phantom, concentric with a circular uniform collimated light source. The photon detector was configured to only detect photons exiting the simulation box, so did not detect photons directly emitted from the light source. Simulations were performed for wavelengths from 400 to 700nm, in steps of 20nm with at least 4 million photons at each wavelength.

Vessels were simulated as cylinders. The molar extinction coefficient for haemoglobin was taken from the data tabulated in [29] and a combined extinction coefficient was produced assuming 98% oxygen saturation. The haemoglobin concentration was adjusted for the approximate Fåhræus effect [18]. To perform this adjustment, for each blood haemoglobin concentration at each diameter, the haematocrit (H_f) was estimated using the three-fold conversion, which suggests there is approximately a 3% increase in haematocrit per 1g/dL haemoglobin [30], [31] – although there are some doubts as to how exactly this holds, especially with varying participant age [32]. If the vessel diameter was greater than 25µm, the haematocrit of the vessel H_v was defined in terms of the original haematocrit H_f and the diameter D as per Eq. (3) [33], [34].

$$\left.H_v\right/_{H_f} = H_f + (1 - H_f)(1 + 1.7e^{-0.35D} - 0.6e^{-0.011D}) \quad (3)$$

When the vessel diameter was under 25µm, then the haematocrit was estimated by linear interpolation between the values in Table 1, which were estimated based on information in [35] and (3).

TABLE I. HAEMATOCRIT CORRECTION FACTORS

Diameter (µm)	$\left.H_v\right/_{H_f}$
2.6	1
3.3	0.936
11	0.671
25	Value from Eq. (3)

After this adjustment to haemoglobin concentration, μ_S was calculated by taking the tabulated μ_S values from [36] for 45% haematocrit at 98% oxygen saturation, and then adjusting for the haematocrit using equation 13 from [36], reproduced below as Eq. (4) and Eq. (5), where H_t is the haematocrit in the target vessel, and H_s is the haematocrit in the reference sample from [36].

$$\mu_s(H_t, \lambda) = \frac{\gamma(t)}{\gamma(H_s)} \frac{H_t}{H_s} \mu_s(H_s, \lambda) \quad (4)$$

$$\gamma(H) \approx (1 - H)^2 \quad (5)$$

The calculation of μ_A required applying the pigment packaging effect to the adjusted blood haemoglobin concentration. For this, the methods of [36] were used, such that red blood cells were assumed to be cubes with a volume equal to that of a sphere with a diameter of $\sqrt[3]{90}$ µm.

The refractive index for the blood was calculated as per [37] reproduced below as (6). In (6), $\beta(\lambda)$ represents a temperature dependent factor, C represents the concentration of haemoglobin in g/dL, and the refractive index of water is estimated based on [38], which in turn uses the methods of [39] for an assumed temperature of 37 Celsius, a salinity of 0 ppm and a pressure, P, of 1.033 kg/cm^2, reproduced here as Eq. (7).

$$n(C, \lambda) = n_{H_2O}(\lambda)[\beta(\lambda)C + 1] \quad (6)$$

$$n_{H_2O}(\lambda) = 1.3247 + (3.3 \times 10^3)\lambda^{-2} - (3.2 \times 10^7)\lambda^{-4} - (2.5 \times 10^{-6})T^2 + 1.021P(1.45 \times 10^{-5})(1 - 4.5 \times 10^{-3}T) \quad (7)$$

The anisotropy for the blood medium was set to 0.9875, which is approximately in the standard ranges given for visible wavelengths [40], [41]. We assumed that anisotropy for blood was not dependent on wavelength [42].

The sclera absorption and scattering coefficients were taken from [43]. Pigmentation in the sclera was modelled as an equimolar mixture of pheomelanin and eumelanin with spectra taken from [44]. This pigmentation absorption was distributed homogeneously throughout the 'sclera' material, rather than concentrated in melanosomes as would be expected *in vivo* [45].

The exact concentrations of melanin, haemoglobin, and the vessel diameters and depths used for different simulations are given in the results.

B. *Measures of redness*

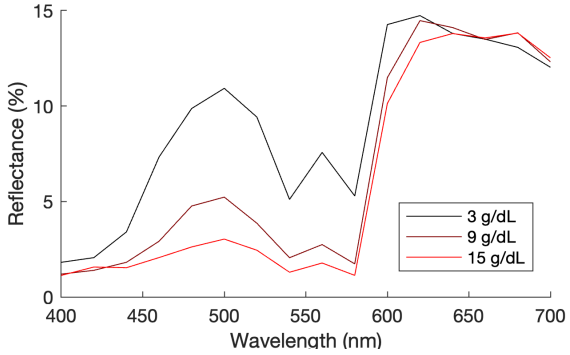

Figure 3. Reflectance spectra for varying haemoglobin concentrations (3, 9, and 15 g/dL) for a 100 µm radius vessel at 100 µm deep in the sclera, with a 0 g/dL melanin concentration, under CIE D65 illumination.

The reflectance spectra for each pixel (examples shown in Fig. 3) were transformed into the CIE 1931 XYZ 2-degree colour space, and then into linearised sRGB colour space with a CIE D65 white point. For this work, the mean *r*-chromaticity was calculated, where the *r*-chromaticity is defined for each pixel from the RGB values as per Eq. (8):

$$r = \frac{R}{R+G+B} \quad (8)$$

Other potential redness measures exist, such as erythema index [46], and this analysis could be repeated with alternative measures.

Images which are displayed in this work are provided in gamma-corrected sRGB colour space for visual inspection.

IV. Results

A. Effect of individual factors on redness of the eye

Visual results are shown in Fig. 4, and numerical results are presented in Fig 5. As well as the mean *r*-chromaticity, which represents an average across the image, these results consider the 99th percentile *r*-chromaticity, which has been used in prior research. The 99th percentile is used because filtering to the reddest areas is functionally a technique to filter to only blood vessels.

Blood haemoglobin concentration: As blood haemoglobin concentration increases, the *r*-chromaticity mean and 99th percentile increase. The rate of increase decreases at higher haemoglobin concentration.

Vessel diameter: As vessel diameter increases, the *r*-chromaticity mean and 99th percentile increase. The rate of increase decreases at higher vessel diameters.

Vessel density: As vessel density increases, the mean *r*-chromaticity increases. The 99th percentile remains approximately constant.

Vessel depth: As vessels lie deeper in the sclera, the *r*-chromaticity mean and 99th percentile decrease. The rate of decrease reduces for deeper vessels, until the *r*-chromaticity tends to the *r*-chromaticity of the sclera with no blood vessel.

Pigmentation in the sclera: As melanin concentration in the sclera increases, the mean *r*-chromaticity increases at a decreasing rate. The 99th percentile *r*-chromaticity decreases.

B. Confusion between factors

Based on the results in part A, it is possible to design situations in which mean *r*-chromaticity across the entire image is the same (0.400 to three decimal places, chosen arbitrarily as an example) but the actual blood haemoglobin concentration varies from severely anaemic (2.5 g/dL) to non-anaemic (15 g/dL). This is illustrated in Fig. 6. These physiological factors – such as vessel diameter – might vary between individuals but might also be impacted by effects such as recent trauma, irritation, or eyedrops.

C. Limitations

The simulations presented in this work are primarily intended to be illustrative of the order of magnitude of the effects, rather than a fully physiologically accurate model. In particular, the simulated vessel has no vessel wall. Vessel wall thickness can be important in the appearance of retinal vessels [47], but there is less evidence on the role of vessel wall thickness in the anterior segment of the eye. It is likely that including vessel walls would not change the general trend of these results, but vessel wall thickness may, in fact, be an additional factor affecting vessel colour/redness.

This work considers the sclera as an example scattering medium. It's likely that similar results – and therefore similar issues with measuring redness – would be experienced when imaging other blood vessels in scattering materials, such as seen on the conjunctiva of the lower eyelid, or to blood vessels within the skin.

(A) Blood haemoglobin concentration ranging from 3 (left) to 15 g/dL (right) in 3 g/dL increments. Vessel radius and vessel depth are 100 μm, and melanin concentration is 0 g/dL.

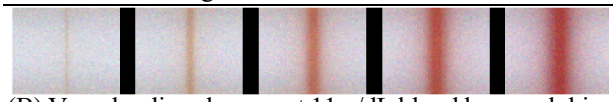

(B) Vessel radius changes at 11 g/dL blood haemoglobin, 0 g/dL melanin. Vessel depth is equal to vessel radius – from left to right, 10, 25, 50, 75, 100 μm.

(C) Vessel density increasing from left to right, at 11 g/dL blood haemoglobin concentration. Vessel depth is 100 μm, vessel radius is 100 μm. The melanin concentration is 0 g/dL. Vessel density decreases are represented by larger unoccupied areas either side of the blood vessel.

(D) Vessel depth changes, with a 100 μm radius, 0 g/dL melanin concentration, and 11 g/dL blood haemoglobin concentration. Vessel depth (from left to right) is 100, 125, 150, 200, 250 μm.

(E) Changes in melanin concentration - from left to right, 0, 0.05, 0.1, 0.2, 0.5 g/dL melanin concentration. All blood vessels are identical, with 11 g/dL blood haemoglobin concentration, 100 μm depth, 100 μm radius.

Figure 4. Effect of physiological factors on appearance of blood vessels: results from simulated scleral blood vessels, shown as sRGB gamma-corrected images for visual interpretation. Black bars represent the edge of images and are used for spacing for clarity for display.

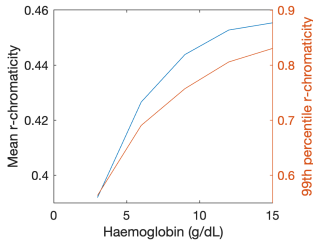

(A) Effect of blood haemoglobin concentration on r-chromaticity. Vessel radius 100 µm, vessel depth 100 µm, and 0 g/dL melanin.

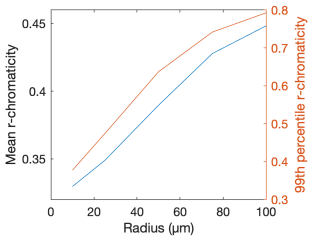

(B) Effect of vessel radius on r-chromaticity. Blood haemoglobin concentration at 11 g/dL, 0 g/dL melanin, and depth equal to vessel radius.

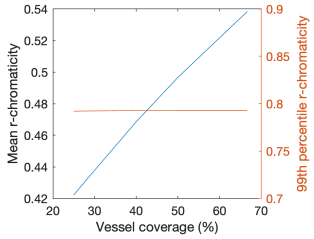

(C) Effect of vessel density (vessel diameter as a proportion of image width) on r-chromaticity. Blood haemoglobin concentration at 11 g/dL, 100 µm radius, 100 µm depth, 0g/dL melanin.

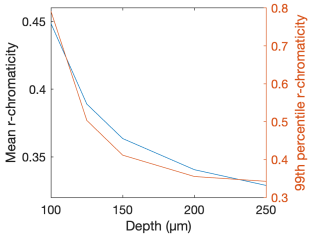

(D) Effect of depth on r-chromaticity. Data collected at haemoglobin concentration of 11 g/dL, 100 µm radius, 0 g/dL melanin.

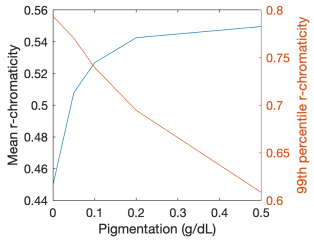

(E) Effect of melanin concentration in the sclera on r-chromaticity. Blood haemoglobin concentration at 11 g/dL, 100 µm radius, and 100 µm depth.

Figure 5. Changes in image *r*-chromaticity as inputs to the tissue colour model change.

V. Conclusion

The simulations show that the same redness metric can be obtained at vastly different haemoglobin concentrations, simply by modulating the structure of the tissue which is simulated. These modulations are likely to be within physiologically reasonable limits. This suggests that inter-person variability might be a potential obstacle to using pallor to judge blood haemoglobin status, and may account for the mixed or poor results seen in prior studies (e.g. [12]). Therefore, when using digital cameras to screen for anaemia using redness, care should be taken to either adjust for, or hold constant, the physiological factors (other than blood haemoglobin concentration) which may influence redness.

Acknowledgment

T.A.W. was supported by the EPSRC Centre for Doctoral Training in Intelligent, Integrated Imaging in Healthcare (i4health), EP/S021930/1. For the purpose of open access, the author has applied a Creative Commons Attribution (CC BY) license to any Author Accepted Manuscript version arising.

(A) Blood haemoglobin concentration 2.35 g/dL, 100 µm radius, 100 µm depth, and 0.005 g/dL melanin.

(B) Blood haemoglobin concentration 11 g/dL, 58 µm radius, 58 µm depth, and 0 g/dL melanin.

(C) Blood haemoglobin concentration 15 g/dL, 100 µm radius, 121 µm depth, and 0g/dL melanin.

(D) Blood haemoglobin concentration 15 g/dL, 49 µm radius, 49 µm depth, and 0 g/dL melanin.

Figure 6. Simulated overhead views of a single blood vessel in the sclera. Each image has the same mean *r*-chromaticity (0.400 to three decimal places, taken across the entire image prior to conversion to sRGB for display) but different underlying physiological factors.

References

[1] A. O. Oladunjoye and Osungbade, Kayode O., 'Anaemia in developing countries: burden and prospects of prevention and control', in *Anaemia*, Edited by Donald Silverberg, 2012, pp. 116–29.

[2] R. K. Rai, W. W. Fawzi, A. Barik, and A. Chowdhury, 'The burden of iron-deficiency anaemia among women in India: how have iron and folic acid interventions fared?', *WHO South-East Asia Journal of Public Health*, vol. 7, no. 1, p. 18, Apr. 2018, doi: 10.4103/2224-3151.228423.

[3] J. Turner, M. Parsi, and M. Badireddy, 'Anemia', in *StatPearls*, Treasure Island (FL): StatPearls Publishing, 2025. Accessed: Jan. 21, 2025. [Online]. Available: http://www.ncbi.nlm.nih.gov/books/NBK499994/

[4] J. P. Chalco, L. Huicho, C. Alamo, N. Y. Carreazo, and C. A. Bada, 'Accuracy of clinical pallor in the diagnosis of anaemia in children: a meta-analysis', *BMC Pediatrics*, vol. 5, no. 1, p. 46, Dec. 2005, doi: 10.1186/1471-2431-5-46.

[5] K. Yurdakök, Ş. N. Güner, and S. S. Yalçın, 'Validity of using pallor to detect children with mild anemia', *Pediatrics International*, vol. 50, no. 2, pp. 232–234, 2008, doi: 10.1111/j.1442-200X.2008.02565.x.

[6] J. Critchley and I. Bates, 'Haemoglobin colour scale for anaemia diagnosis where there is no laboratory: a systematic review', *International Journal of Epidemiology*, vol. 34, no. 6, pp. 1425–1434, Dec. 2005, doi: 10.1093/ije/dyi195.

[7] C. B. Mogensen, J. E. Sørensen, and A. Bjorkman, 'Pallor as a sign of anaemia in small Tanzanian children at different health care levels', *Acta Tropica*, vol. 99, no. 2, pp. 113–118, Oct. 2006, doi: 10.1016/j.actatropica.2005.12.010.

[8] L. Muhe, B. Oljira, H. Degefu, S. Jaffar, and M. W. Weber, 'Evaluation of clinical pallor in the identification and treatment of

children with moderate and severe anaemia', *Tropical Medicine & International Health*, vol. 5, no. 11, pp. 805–810, 2000, doi: 10.1046/j.1365-3156.2000.00637.x.

[9] R. G. Mannino *et al.*, 'Smartphone app for non-invasive detection of anemia using only patient-sourced photos', *Nat Commun*, vol. 9, no. 1, Art. no. 1, Dec. 2018, doi: 10.1038/s41467-018-07262-2.

[10] A. R. Kent, S. H. Elsing, and R. L. Hebert, 'Conjunctival vasculature in the assessment of anemia', *Ophthalmology*, vol. 107, no. 2, pp. 274–277, Feb. 2000, doi: 10.1016/S0161-6420(99)00048-2.

[11] T. A. Wemyss *et al.*, 'Feasibility of smartphone colorimetry of the face as an anaemia screening tool for infants and young children in Ghana', *PLOS ONE*, vol. 18, no. 3, p. e0281736, Mar. 2023, doi: 10.1371/journal.pone.0281736.

[12] T. Wemyss *et al.*, 'Diagnosing anaemia via smartphone colorimetry of the eye in a population of pregnant women', *Physiol. Meas.*, 2025, doi: 10.1088/1361-6579/adab4d.

[13] G. Dimauro, M. G. Camporeale, A. Dipalma, A. Guarini, and R. Maglietta, 'Anaemia detection based on sclera and blood vessel colour estimation', *Biomedical Signal Processing and Control*, vol. 81, p. 104489, Mar. 2023, doi: 10.1016/j.bspc.2022.104489.

[14] M. Shahidi, J. Wanek, B. Gaynes, and T. Wu, 'Quantitative Assessment of Conjunctival Microvascular Circulation of the Human Eye', *Microvasc Res*, vol. 79, no. 2, pp. 109–113, Mar. 2010, doi: 10.1016/j.mvr.2009.12.003.

[15] Z. Rusavy, B. Pitrova, V. Korecko, and V. Kalis, 'Changes in capillary diameters in pregnancy-induced hypertension', *Hypertens Pregnancy*, vol. 34, no. 3, pp. 307–313, 2015, doi: 10.3109/10641955.2015.1033925.

[16] J. R. Levick and C. C. Michel, 'The effects of position and skin temperature on the capillary pressures in the fingers and toes', *The Journal of Physiology*, vol. 274, no. 1, pp. 97–109, 1978, doi: 10.1113/jphysiol.1978.sp012136.

[17] L. N. M. Duyens, 'The flattering of the absorption spectrum of suspensions, as compared to that of solutions', *Biochimica et Biophysica Acta*, vol. 19, pp. 1–12, Jan. 1956, doi: 10.1016/0006-3002(56)90380-8.

[18] R. Fåhræus and T. Lindqvist, 'THE VISCOSITY OF THE BLOOD IN NARROW CAPILLARY TUBES', *American Journal of Physiology-Legacy Content*, vol. 96, no. 3, pp. 562–568, Mar. 1931, doi: 10.1152/ajplegacy.1931.96.3.562.

[19] R. Fåhraeus, 'Die Strömungsverhältnisse und die Verteilung der Blutzellen im Gefässystem', *Klin Wochenschr*, vol. 7, no. 3, pp. 100–106, Jan. 1928, doi: 10.1007/BF01738786.

[20] M. M. Park, B. K. Young, L. L. Shen, R. A. Adelman, and L. V. Del Priore, 'Topographic Variation of Retinal Vascular Density in Normal Eyes Using Optical Coherence Tomography Angiography', *Transl Vis Sci Technol*, vol. 10, no. 12, p. 15, Oct. 2021, doi: 10.1167/tvst.10.12.15.

[21] Y. Komai and T. Ushiki, 'The three-dimensional organization of collagen fibrils in the human cornea and sclera.', *Investigative Ophthalmology & Visual Science*, vol. 32, no. 8, pp. 2244–2258, Jul. 1991.

[22] D. J. Maggs, P. E. Miller, and R. Ofri, *Slatter's Fundamentals of Veterinary Ophthalmology*. Elsevier Health Sciences, 2017.

[23] T. Akagi *et al.*, 'Conjunctival and Intrascleral Vasculatures Assessed Using Anterior Segment Optical Coherence Tomography Angiography in Normal Eyes', *American Journal of Ophthalmology*, vol. 196, pp. 1–9, Dec. 2018, doi: 10.1016/j.ajo.2018.08.009.

[24] R. Russell, J. R. Sweda, A. Porcheron, and E. Mauger, 'Sclera color changes with age and is a cue for perceiving age, health, and beauty', *Psychology and Aging*, vol. 29, no. 3, pp. 626–635, 2014, doi: 10.1037/a0036142.

[25] T. J. Liesegang, 'Pigmented Conjunctival and Scleral Lesions', *Mayo Clinic Proceedings*, vol. 69, no. 2, pp. 151–161, Feb. 1994, doi: 10.1016/S0025-6196(12)61042-8.

[26] S. Yan and Q. Fang, 'Hybrid mesh and voxel based Monte Carlo algorithm for accurate and efficient photon transport modeling in complex bio-tissues', *Biomed. Opt. Express, BOE*, vol. 11, no. 11, pp. 6262–6270, Nov. 2020, doi: 10.1364/BOE.409468.

[27] S. Yan, S. L. Jacques, J. C. Ramella-Roman, and Q. Fang, 'Graphics-processing-unit-accelerated Monte Carlo simulation of polarized light in complex three-dimensional media', *JBO*, vol. 27, no. 8, p. 083015, May 2022, doi: 10.1117/1.JBO.27.8.083015.

[28] Q. Fang and D. A. Boas, 'Monte Carlo Simulation of Photon Migration in 3D Turbid Media Accelerated by Graphics Processing Units', *Opt. Express, OE*, vol. 17, no. 22, pp. 20178–20190, Oct. 2009, doi: 10.1364/OE.17.020178.

[29] S. Prahl, 'Optical Absorption of Hemoglobin', Oregon Medical Laser Center. Accessed: Dec. 19, 2022. [Online]. Available: https://omlc.org/spectra/hemoglobin/index.html

[30] B. J. Bain, I. Bates, and M. A. Laffan, *Dacie and Lewis Practical Haematology E-Book: Dacie and Lewis Practical Haematology E-Book*. Elsevier Health Sciences, 2016.

[31] -Ryalat Nosaiba Al, S. A. AlRyalat, L. W. Malkawi, -Hassan Hana Abu, O. Samara, and A. Hadidy, 'The haematocrit to haemoglobin conversion factor: A cross-sectional study of its accuracy and application', *New Zealand Journal of Medical Laboratory Science*, vol. 72, no. 1, pp. 18–21, Nov. 2020, doi: 10.3316/informit.511877744440733.

[32] L. Quintó *et al.*, 'Relationship between haemoglobin and haematocrit in the definition of anaemia', *Tropical Medicine & International Health*, vol. 11, no. 8, pp. 1295–1302, 2006, doi: 10.1111/j.1365-3156.2006.01679.x.

[33] A. R. Pries, D. Neuhaus, and P. Gaehtgens, 'Blood viscosity in tube flow: dependence on diameter and hematocrit', *American Journal of Physiology-Heart and Circulatory Physiology*, vol. 263, no. 6, pp. H1770–H1778, Dec. 1992, doi: 10.1152/ajpheart.1992.263.6.H1770.

[34] A. Farina, A. Fasano, and F. Rosso, 'A theoretical model for the Fåhræus effect in medium–large microvessels', *Journal of Theoretical Biology*, vol. 558, p. 111355, Feb. 2023, doi: 10.1016/j.jtbi.2022.111355.

[35] K. H. Albrecht, P. Gaehtgens, A. Pries, and M. Heuser, 'The Fahraeus effect in narrow capillaries (i.d. 3.3 to 11.0 μm)', *Microvascular Research*, vol. 18, no. 1, pp. 33–47, Jul. 1979, doi: 10.1016/0026-2862(79)90016-5.

[36] N. Bosschaart, G. J. Edelman, M. C. G. Aalders, T. G. van Leeuwen, and D. J. Faber, 'A literature review and novel theoretical approach on the optical properties of whole blood', *Lasers Med Sci*, vol. 29, no. 2, pp. 453–479, Mar. 2014, doi: 10.1007/s10103-013-1446-7.

[37] M. Friebel and M. Meinke, 'Model function to calculate the refractive index of native hemoglobin in the wavelength range of 250-1100 nm dependent on concentration', *Appl. Opt., AO*, vol. 45, no. 12, pp. 2838–2842, Apr. 2006, doi: 10.1364/AO.45.002838.

[38] H. Buiteveld, J. H. M. Hakvoort, and M. Donze, 'Optical properties of pure water', in *Ocean Optics XII*, SPIE, Oct. 1994, pp. 174–183. doi: 10.1117/12.190060.

[39] G. T. McNeil, 'Metrical Fundamentals of Underwater Lens System', *OE*, vol. 16, no. 2, pp. 128–139, Apr. 1977, doi: 10.1117/12.7972089.

[40] M. Hammer, A. N. Yaroslavsky, and D. Schweitzer, 'A scattering phase function for blood with physiological haematocrit', *Phys. Med. Biol.*, vol. 46, no. 3, p. N65, Mar. 2001, doi: 10.1088/0031-9155/46/3/402.

[41] D. K. Sardar and L. B. Levy, 'Optical Properties of Whole Blood', *Lasers Med Sci*, vol. 13, no. 2, pp. 106–111, Jun. 1998, doi: 10.1007/s101030050062.

[42] A. Roggan, M. Friebel, K. Doerschel, A. Hahn, and G. J. Mueller, 'Optical properties of circulating human blood in the wavelength range 400-2500 nm', *JBO*, vol. 4, no. 1, pp. 36–46, Jan. 1999, doi: 10.1117/1.429919.

[43] M. Hammer, A. Roggan, D. Schweitzer, and G. Muller, 'Optical properties of ocular fundus tissues-an in vitro study using the double-integrating-sphere technique and inverse Monte Carlo simulation', *Phys. Med. Biol.*, vol. 40, no. 6, p. 963, Jun. 1995, doi: 10.1088/0031-9155/40/6/001.

[44] 'Extinction Coefficient of Melanin'. Accessed: Jan. 06, 2025. [Online]. Available: https://omlc.org/spectra/melanin/extcoeff.html

[45] D.-N. Hu, J. D. Simon, and T. Sarna, 'Role of ocular melanin in ophthalmic physiology and pathology', *Photochem Photobiol*, vol. 84, no. 3, pp. 639–644, 2008, doi: 10.1111/j.1751-1097.2008.00316.x.

[46] T. Yamamoto, H. Takiwaki, S. Arase, and H. Ohshima, 'Derivation and clinical application of special imaging by means of digital cameras and Image J freeware for quantification of erythema and pigmentation', *Skin Research and Technology*, vol. 14, no. 1, pp. 26–34, 2008, doi: 10.1111/j.1600-0846.2007.00256.x.

[47] E. Di Marco *et al.*, 'A literature review of hypertensive retinopathy: systemic correlations and new technologies', 2022, doi: 10.26355/eurrev_202209_29742.